Mapping vegetation in urban areas using Sentinel-2

Oladimeji Mudele, Paolo Gamba*
Department of Electrical, Computer and Biomedical Engineering
University of Pavia
Pavia, Italy
*Corresponding author: gamba@unipv.it

***Abstract*— The rapid expansion of cities globally leads to new challenges related to quality of life and health. The presence and fractional distribution of vegetation within urban cities directly impact the life and health of urban dwellers. This paper presents an approach to map urban vegetation from Sentinel-2 data. The twin Sentinel-2 satellites offer a 5-day revisit time global coverage at unprecedented spatial and temporal resolution. The temporal resolution allows for seasonal aggregation of the input data, thus providing phenological information. By considering seasonally aggregated Normalized Difference Spectral Vector (NDSV), a classification was performed using Random Forest (RF) and compared with Classification and Regression Trees (CART) and Support Vector Machines (SVM).**

Keywords—urban remote sensing, vegetation mapping, risk mapping

I. INTRODUCTION

Urban areas are characterized by relatively dense population, human activities and a complex intertwine of artificial and natural environments. Many of the world's urban cities are becoming congested. Resulting from the rapid expansion and congestion of urban cities is the rise of unplanned areas with skewed ecological balance between artificial and natural landcovers, thus affecting the lives of urban dwellers. These factors, along with the recent increase in availability of Earth Observation data, caused an increased number of global studies of urban environments [1] [2].

Urban green spaces impact the urban ecosystem from the standpoints of health and quality of life. Vegetation may vary in height, sizes, canopy, and species, with each of these variations resulting in a different environmental impact. Major parts of urban areas where vegetations are often found include parks, Government reserved areas, river banks, domestic gardens, and street trees. Their impacts include pollution removal, noise attenuation, wind storm control, temperature reduction, ground water replenishment, and recreation for citizens. It is therefore important to study the quality and presence of vegetation in urban areas. Urban vegetation maps are needed in various applications and studies to improve the lives of urban dwellers [3].

A major application of interest is in the field of Landscape Epidemiology. Here, urban vegetation maps obtained from Earth Observation data are combined with other environmental variables to model the spread of diseases in urban environments. A major specific application in this domain is in developing models for Mosquito borne diseases spread; Zika, Dengue, Chikungunya viruses etc. Previous studies have shown a relationship between local moisture supply, vegetation canopy structure and the abundance of mosquitoes. Fully developed tree canopies provide shades that reduce evaporation from containers of mosquito larvae and shield the vector habitat from wind. Vegetation condition also provide proxy to moisture and precipitation, vital variables for the survival of mosquito species [4] [5].

Recent studies about Zika, Dengue and similar disease spread models rely on remote sensing data such as MODIS Normalized difference vegetation index (NDVI) and Enhanced Vegetation Index (EVI) layers in the MOD13Q1 NASA product. With a spatial resolution of 250 meters, these layers do not provide adequate details required to delineate the complexity of urban land covers [6]. Maps obtained using NDVI or EVI do not provide information about the size and structure of the vegetation, important factors for vector survival and subsequent environmental suitability for vector-borne diseases. Other features, such as the Tasseled cap brightness, greenness and wetness, have been used to generate proxies to vegetation quality using Landsat TM data. However, this approach too shows some of the drawbacks earlier stated [7]. The use of higher spatial resolution data including SPOT (Satellite Pour l'Observation de la Terre) dataset has alternatively been explored to obtain local scale urban vegetation maps to be included in disease spread models [5]. However, this dataset is not available for free, and thus not publicly suited for research studies.

In this study, we present a procedure to extract urban vegetations from Sentinel-2 (S-2) multispectral data. S-2 data provide novel spectral capabilities with 13 spectral bands (e.g. 3 bands in red-edge and 2 bands in SWIR) at up to 10-meter spatial resolution. The 5-day global revisit time (due to 2 satellites 180° apart in orbit) provides enough temporal information to incorporate phenological information into the urban vegetation mapping procedure. In the following, we present results for urban vegetation mapping based on the Normalized Difference Spectral Vector (NDSV) input. For this purpose, a robust classifier - Random Forest (RF) -was applied and compared with Classification and Regression Trees (CART) and Support Vector Machines (SVM).

II. THE PROCESSING CHAIN

To mitigate errors in the data due to atmosphere and sensor acquisition parameters, there is the need for data calibration, co-registration of overlapping scenes, and cloud cover filtering to select images suitable for the procedure. These steps were already implemented in the cloud computing platform used in this work (Google Earth Engine). Scene combination (in case of using multiple overlapping data) and/or selection (in case of using single image input) was thus the only pre-processing step performed.

To map vegetation within an urban area, it is important to define the urban boundary. The procedure implemented for this work includes an initial semi-automatic urban area extraction in the area of interest. Then, a buffer zone around the extracted urban extent is obtained and used as geographical bound for the urban vegetation mapping procedure. A full description of the processing chain is shown in fig. 1.

A. Urban extent extraction

A semi-supervised urban extent extraction procedure

based on the normalized difference spectral vector [8] was used in this work. Our implementation of this procedure takes a single S-2 data as input (the least cloudy in the year of interest), applies the NDSV transformation as defined in [9], and selects training points automatically from the urban class of the GlobCover product, a coarser (300m spatial resolution) global landcover map. The output map is then spatially regularized using a morphological filter.

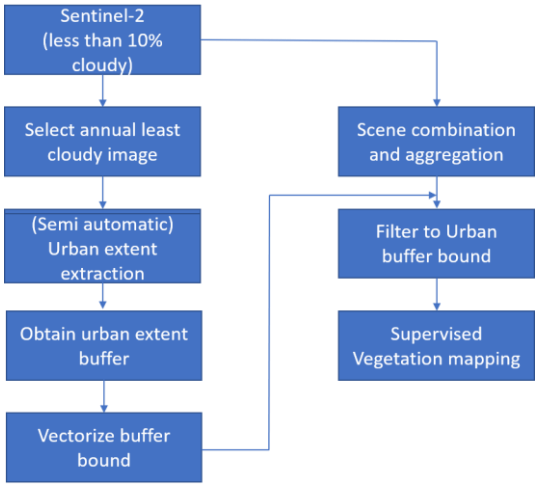

Fig. 1. Proposed urban vegetation mapping processing chain

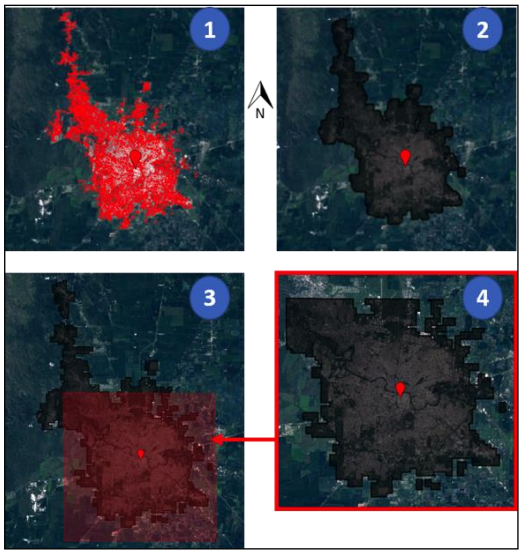

Fig. 2. Semi-automatic urban mapping and buffer mask extraction procedure. Steps are as follow: 1- extraction of urban extents; 2- buffer application using a morphological dilation; 3- sub-area extraction; 4- final result.

Since our interest is the boundary of the urban area plus its fringes, a buffer around the resulting map is obtained using a dilate morphological operation. The boundary of this buffer is vectorized to produce the final urban area plus fringes boundary. An example for the city of Cordoba (Argentina) is shown in fig. 2.

B. Vegetation mapping

Vegetation mapping is then performed inside the urban and peri-urban areas by means of supervised classification. As with every supervised procedure, the final map quality depends on the selection of the representative samples used to train the classifier. These points have been mostly collected by field visit, but integrated by looking at high-resolution aerial images. Constraints considered in selecting the classification legend include spatial scale of data, season of the year when points are collected and, more importantly, the goals of the work. Based on these constraints, the following classes were defined: Trees, Bushes, Grass, Water, Artificial surfaces, and Bare soil.

To obtain a single image for classification input, multitemporal Sentinel-2 images overlapping over the same scene were combined by means of greenest pixel compositing, i.e. by selecting for each pixel the spectrum from the scene with the largest NDVI. This combination was done annually, seasonally and bi-monthly. There are two major motivations for considering seasonal/bi-monthly aggregation. First, vegetations behave dynamically across different times of the year. Seasonal and bi-monthly aggregation incorporates this phenological behavior/changes across all seasons in the spectra description of the vegetations. Second, annual greenest pixels could still contain cloudy pixels. However, it is most unlikely for the same pixel to be cloudy across all seasons of the year.

In the seasonal and bi-monthly cases, the output seasonal greenest pixel mosaics are stacked to produce a single dataset. Then, to remove the errors due to differences in the acquisitions across the different images in the input collection, the composited data is converted to the above mentioned NDSV feature. In the cases of seasonal and bi-monthly aggregation, the NDSV is computed for each of the output mosaics before aggregation. Results obtained with NDSV input are benchmarked against using only the original spectral features.

As for the classifier, Random Forest (RF) was selected for this work, due to its robustness with respect to the quality of training samples, as well as its robustness against unbalanced data and overfitting [10] [11]. To justify this choice, RF was tested in comparison to other state-of-the-art classifiers: CART and SVM.

III. Experimental Results

The proposed methodology was tested with data covering the city of Cordoba, Argentina, located at 31º24’30’’ S, 64 º11’02’’ W. Cordoba covers an area of 576km^2 with a population of nearly 1.5 million [12].

Sentinel-2 dataset within one-year (Sept. 2017 to Aug. 2018) were considered. After selecting images with less than 10% cloud cover, 51 images were retained and combined. 10 of the 13 bands in S-2 images, i.e. those giving information about land covers were selected for this work, discarding specifically the Aerosol, Cirrus and Water vapor bands. This resulted in a 10 spectral band single input image for the annual greenest pixel composite – 40 bands and 60 bands in the seasonal and bi-monthly aggregates respectively. For the NDSV feature, a 45-band feature was obtained from the annual greenest, 180 bands for seasonal aggregate and 270 bands for bi-monthly aggregate.

Field visits were made to select points representative of the Trees, Bushes, Grass, Water and Bare soil classes. Points for the artificial surfaces class were selected instead by visual inspection of Google Earth™ images. A total of 1,428 points covering all classes were collected. A major limitation of the points collected is their geographical distribution (see fig. 3). This occurred due to constraints including inaccessibility of many areas. Thus, the training of the classifier and validation

of the resulting model was only done on points taken within the areas that could be accessed.

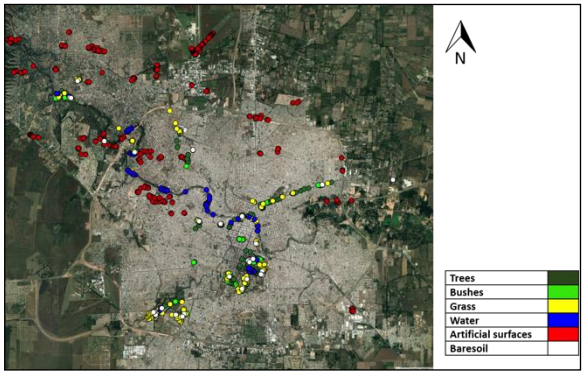

Fig. 3. Landsat view of the city of Cordoba with the selected training and validation points overlaid.

A. *Vegetation maps*

The obtained vegetation maps were evaluated with respect to the Overall accuracy (O.A.), Kappa coefficient, Producer accuracy and User accuracy [13]. 20-fold cross-validation was used to ensure unbiased accuracy values. From the performed experiments, the RF classifier demonstrates a larger robustness to limitations in the number of training samples, with only marginal improvement shown in classification accuracy by varying the proportion of sample points used for training. Model parameters were tuned to find the optimal values – "Number of trees" for RF (see fig. 4) and "type of kernel function" for SVM (see fig. 5). The results show that RF (100 trees) produces better classification accuracy values than CART or SVM. The results for all these tests are reported in Table I.

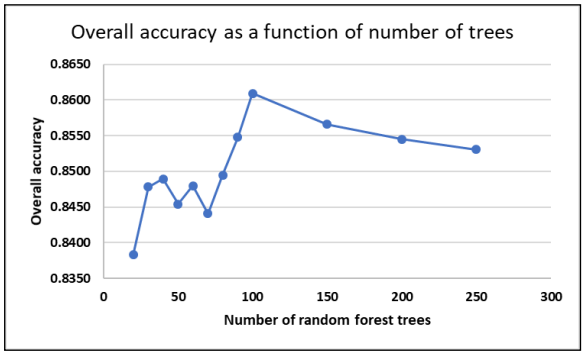

Fig. 4. Plot of overall accuracy of classification as a function of number of Random Forest trees.

As shown in Table I, seasonal aggregations improve the accuracy of the classification map. This is specifically seen in the lower confusion between Bushes and Grass. Since it is difficult to find pure bush pixels at 10 m spatial resolution, the phenological information provided in seasonal aggregation improves the separability between the classes. Bi-monthly aggregations, instead, do not provide additional improvement with respect to seasonal to justify the resulting increase in computational complexity.

TABLE I. CLASSIFICATION RESULTS FOR SPECTRAL INPUT

RF (100 trees) – Spectral annual greenest feature input						
	Trees	Bushes	Grass	Water	Artificial	Bare soil
Prod	0.781	0.523	0.727	0.734	0.973	0.193
User	0.690	0.805	0.681	0.783	0.931	0.708
O.A	0.826 ± 0.019					
Kappa	0.746 ± 0.026					
RF (100 trees) – Spectral seasonal aggregated feature input						
	Trees	Bushes	Grass	Water	Artificial	Bare soil
Prod	0.841	0.577	0.756	0.814	0.983	0.453
User	0.746	0.878	0.759	0.862	0.935	0.821
O.A	0.861 ± 0.020					
Kappa	0.800 ± 0.026					
RF (100 trees) – Spectral bi-monthly aggregated feature input						
	Trees	Bushes	Grass	Water	Artificial	Bare soil
Prod	0.839	0.602	0.744	0.810	0.987	0.335
User	0.764	0.864	0.785	0.815	0.928	0.913
O.A	0.862 ± 0.020					
Kappa	0.800 ± 0.026					
CART – Spectral seasonal aggregated feature input						
	Trees	Bushes	Grass	Water	Artificial	Bare soil
Prod	0.639	0.652	0.596	0.745	0.933	0.395
User	0.665	0.564	0.618	0.720	0.946	0.348
O.A	0.778 ± 0.016					
Kappa	0.685 ± 0.023					
SVM (Kernel: Polynomial order 5) – Spectral seasonal aggregated feature input						
	Trees	Bushes	Grass	Water	Artificial	Bare soil
Prod	0.781	0.360	0.641	0.880	0.956	0.407
User	0.671	0.534	0.734	0.708	0.957	0.606
O.A	0.812 ± 0.020					
Kappa	0.730 ± 0.027					

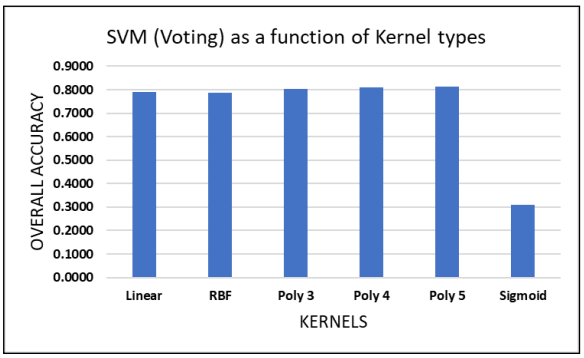

Fig. 5. Classification accuracy results using different kernel functions in the SVM classifier ("Poly #" = Polynomial function of order #).

TABLE II. CLASSIFICATION EVALUATION RESULTS FOR NDSV SEASONAL AGGREGATED FEATURE INPUT

	Trees	Bushes	Grass	Water	Artificial	Bare soil
Prod	0.849	0.535	0.771	0.806	0.979	0.240
User	0.732	0.870	0.755	0.856	0.929	0.779
O.A	0.853 ± 0.019					
Kappa	0.786 ± 0.018					

Even though the NDSV does not quantitatively show better classification result than spectral input (see Table II), the differences are not statistically relevant. As a matter of fact, a comparison of the maps obtained with Spectral and NDSV input shows otherwise. Indeed, they show that NDSV produces better results, especially with respect to mapping vegetation cover (see fig. 7). This disparity between quantitative and qualitative measure is a result of the limitation in geographical distribution of the training data. The classification map obtained using seasonally aggregated NDSV feature is shown in fig. 6. Fig. 7 highlights portions of

the map showing better separation between Trees and Grass classes as obtained using seasonally aggregated NDSV input.

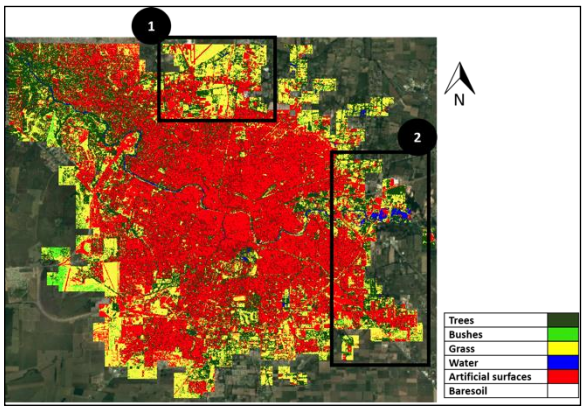

Fig. 6. Classification result obtained with seasonally aggregated NDSV feature and RF classifier (100 trees).

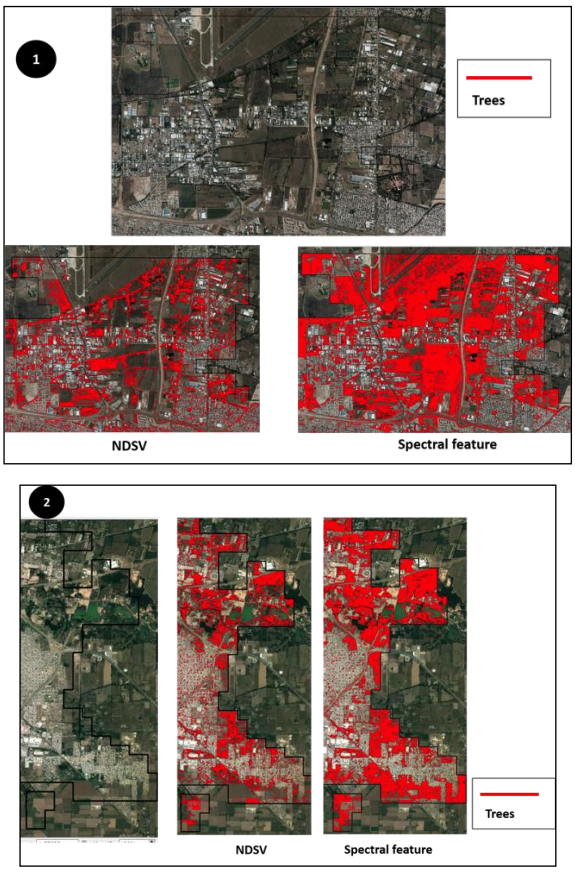

Fig. 7. Qualitative comparison between NDSV and Spectral feature input results for the "Trees" class in selected portions of the urban area.

IV. Conclusions

This study presents a methodology for mapping urban vegetation from Sentinel-2 data, exploiting their high temporal resolution to create seasonally aggregated inputs. Also, NDSV features were compared with spectral features, and the RF classifier with SVM and CART classification models. We found that seasonally aggregated inputs show better performance than annual aggregates for the task at hand, while NDSV improves the separation between Trees and Grass.

A major limitation to the current approach is in the geographical distribution of the training and validation point samples. Moreover, more vegetation classes could have been defined. Further studies will be conducted to mitigate these limitations.

Acknowledgment

The first author gratefully acknowledges the financial support by the European Commission through Horizon 2020 research and innovation programme, grant agreement No 734541 - Project "EOXPOSURE". The authors also acknowledge the contributions of Universidad Nacional de Cordoba in the field observations, and particularly Prof. Marcelo Scavuzzo.

References

[1] M. L. Monika, D. M. Styers, and M. Halabisky. "Monitoring urban tree cover using object-based image analysis and public domain remotely sensed data," Remote Sensing., vol. 3, no. 10, pp. 2243-2262, 2011.

[2] A. Marina. "The effects of urban patterns on ecosystem function," International regional science review., vol. 28, no. 2, pp. 168-192, April 2005

[3] J. R Wolch, J. Byrne, and J. P. Newell, "Urban green space, public health, and environmental justice: The challenge of making cities 'just green enough'," Landscape and urban planning., vol. 125, pp. 234-244, May 2014.

[4] J. P. Messina., M.U. Kraemer, O. J. Brady, D. M. Pigott, F. M. Shearer, D. J. Weiss, N. Golding, C. W. Ruktanonchai, P. W. Gething, E. Cohn, and J. S. Brownstein, "Mapping global environmental suitability for Zika virus," Elife 5: e15272, April 2016.

[5] M. O. Espinosa, D. Weinberg, C. H. Rotela, F. Polop, M. Abril, and C. M. Scavuzzo, "Temporal dynamics and spatial patterns of Aedes aegypti breeding sites, in the context of a dengue control program in Tartagal (Salta province, Argentina)," PLoS neglected tropical diseases: e0004621., vol. 10, no. 5, May 2016.

[6] A. German, M. Espinosa, M. Abril, and C. M. Scavuzzo, "Exploring satellite based temporal forecast modelling of Aedes aegypti oviposition from an operational perspective," Remote Sensing Applications: Society and Environment, vol. 11, pp. 231-240, Aug. 2018.

[7] C. Rotela, F. Fouque, M. Lamfri, P. Sabatier, V. Intrini, M. Zaidenberg, C. Scavuzzo, "Space–time analysis of the dengue spreading dynamics in the 2004 Tartagal outbreak, Northern Argentina," Acta tropica, vol. 103, no. 1, pp. 1-13, July 2007.

[8] T. Giovanna, G. Lisini, E. Angiuli, E. A. Moreno, P. Dondi, A. Gaggia, and P. Gamba, "Scaling up to national/regional urban extent mapping using Landsat data," IEEE Journal of Selected Topics in Applied Earth Observations and Remote Sensing., vol. 8, no. 7, pp. 3710-3719, 2015.

[9] Angiuli, Emanuele, and Giovanna Trianni. "Urban mapping in Landsat images based on normalized difference spectral vector." IEEE Geoscience and Remote Sensing Letters., vol 11, no. 3, pp. 661-665, Mar. 2014.

[10] P. Mahesh, "Random forest classifier for remote sensing classification," International Journal of Remote Sensing., vol. 26, no. 1 (2005): pp. 217-222, January 2005.

[11] B. Mariana, and L. Drăguț, "Random forest in remote sensing: A review of applications and future directions," ISPRS Journal of Photogrammetry and Remote Sensing., vol. 114, pp. 24-31, 2016.

[12] C. Rotela, L. Lopez, M. F. Céspedes, G. Barbas, A. Lighezzolo, X. Porcasi, M. A. Lanfri, C. M. Scavuzzo, and D. E. Gorla, "Analytical report of the 2016 dengue outbreak in Córdoba city, Argentina," Geospatial health., vol. 12, no. 2, 2017.

[13] I. F. J Lucas, F. Janssen, and F. J. van der Wel, "Accuracy assessment of satellite derived landcover data: A review," Photogrammetric Engineering & Remote Sensing, vol. 60, no. 4, pp. 479-426, 1994.